Research Article

EASL EUROPEAN ASSOCIATION FOR THE STUDY OF THE LIVER | JOURNAL OF HEPATOLOGY

Hepatic insulin resistance is associated with increased apoptosis and fibrogenesis in nonalcoholic steatohepatitis and chronic hepatitis C

Carmelo García-Monzón[1,5], Oreste Lo Iacono[2], Rafael Mayoral[3,5], Águeda González-Rodríguez[3,6], María E. Miquilena-Colina[1,5], Tamara Lozano-Rodríguez[1,5], Leonor García-Pozo[1,5], Javier Vargas-Castrillón[1,5], Marta Casado[4,5], Lisardo Boscá[3,5], Ángela M. Valverde[3,6,*,†], Paloma Martín-Sanz[3,5,**,†]

[1]*Liver Research Unit, Hospital Universitario Santa Cristina, Instituto de Investigación Sanitaria Princesa, Madrid, Spain;* [2]*Gastroenterology Unit, Hospital del Tajo, Aranjuez, Madrid, Spain;* [3]*Instituto de Investigaciones Biomédicas "Alberto Sols", Consejo Superior de Investigaciones Científicas, Universidad Autónoma de Madrid (IIBM-CSIC-UAM), Madrid, Spain;* [4]*Instituto de Biomedicina de Valencia, IBV-CSIC, Valencia, Spain;* [5]*Centro de Investigación Biomédica en Red de Enfermedades Hepáticas y Digestivas (CIBERehd), Spain;* [6]*Centro de Investigación Biomédica en Red de Diabetes y Enfermedades Metabólicas Asociadas (CIBERdem), Spain*

Background & Aims: We aimed to elucidate whether hepatic insulin resistance may contribute to hepatocyte apoptosis and fibrogenesis in nonalcoholic fatty liver disease (NAFLD) and in chronic hepatitis C virus (HCV) infection.

Methods: Twenty-seven nonalcoholic steatosis (NAST), 24 nonalcoholic steatohepatitis (NASH), 71 HCV, and 29 patients with histological normal liver (NL) were studied. Real-time PCR, the TUNEL assay, and Western blots were used to assess insulin-signaling molecules, hepatocyte apoptosis, antiapoptotic mediators, active caspase 3, and type I collagen in liver biopsies. HCV core-transfected human hepatocytes were used as an *in vitro* model.

Results: In NAFLD patients, hepatic levels of insulin receptor substrate (IRS) 1, IRS2 2, the p85α subunit of phosphatidylinositol 3-kinase (p85α), phosphorylated protein kinase B (pAkt), phosphorylated forkhead box-containing protein O subfamily-1 (FoxO), and phosphorylated 5′ adenosine monophosphate-activated protein kinase (pAMPK) as well as the antiapoptotic mediators B-cell lymphoma 2 protein (Bcl-2) and myeloid cell leukemia protein-1 (Mcl-1) were significantly lower in NASH than in NAST and NL. Furthermore, hepatocyte apoptosis and increased active caspase 3 were only present in NASH. In HCV patients, hepatic insulin signaling was markedly impaired, regardless of viral genotype and the presence of steatosis paralleled with enhanced apoptosis. In cultured human hepatocytes, HCV core protein decreased pAkt and increased phosphorylation of c-Jun N-terminal kinase (JNK). This effect was more pronounced in lipid-loaded hepatocytes.

Conclusions: Hepatic insulin signaling is impaired in NASH and HCV patients, and downregulation of insulin-sensitive targets is associated with increased apoptosis and fibrogenesis in both conditions. JNK might be a target for HCV-induced insulin resistance.

Keywords: Insulin resistance; Nonalcoholic fatty liver disease; Hepatitis C virus; Apoptosis; Fibrogenesis.

Received 19 January 2010; received in revised form 6 May 2010; accepted 8 June 2010; available online 27 August 2010

* Corresponding author. Address: Instituto de Investigaciones Biomédicas "Alberto Sols" IIBM, CSIC-UAM, Arturo Duperier, 4, 28029 Madrid, Spain.

** Corresponding author. Address: Instituto de Investigaciones Biomédicas "Alberto Sols" IIBM, CSIC-UAM, Arturo Duperier, 4, 28029 Madrid, Spain. Fax: +34 91 4972748.

E-mail addresses: avalverde@iib.uam.es (Á.M. Valverde), pmartins@iib.uam.es (P. Martín-Sanz).

† These two authors share senior authorship.

Abbreviations: Akt, protein kinase B; AMPK, 5′ adenosine monophosphate-activated protein kinase; AST, aspartate aminotransferase; ALT, alanine aminotransferase; Bcl-2, B-cell lymphoma 2 protein; CHL, Chang human liver cells; DGAT, diglycerol acyltransferase; ECHS1, enoyl-CoA hydratase; ECM, extracellular matrix; FoxO1, forkhead box-containing protein O subfamily-1; HCV, hepatitis C virus; HOMA, homeostatic model assessment; HSC, hepatic stellate cell; IR, insulin resistance; IRS, insulin receptor substrate; JNK, c-Jun N-terminal kinase; Mcl-1, myeloid cell leukemia protein-1; NAFLD, nonalcoholic fatty liver disease; NASH, nonalcoholic esteatohepatitis; NAST, nonalcoholic steatosis; NF-κB, nuclear factor kappa B; NL, normal liver; PNPLA3, patatin-like phospholipase domain containing 3; PI3K, phosphatidylinositol 3-kinase; qPCR, quantitative real-time polymerase chain reaction; TNF, tumor necrosis factor; TRAIL, tumor necrosis factor-related apoptosis-inducing ligand; TUNEL, terminal deoxynucleotidyl-transferase-mediated dUTP nick-end labelling.

Introduction

Nonalcoholic fatty liver disease (NAFLD) and chronic hepatitis C virus (HCV) infection are the commonest causes of chronic liver disease in Western countries [1,2]. A number of epidemiologic and clinical studies have shown a close association between fatty liver and insulin resistance (IR) [3,4]. The physiopathological consequences of IR depend on whether the impairment of insulin receptor signaling is in peripheral tissues or in the liver. In peripheral tissues, IR maintains the activity of the hormone-sensitive lipase, increasing free fatty acids in the plasma and

reaching the liver [5]. On the other hand, the main consequence of hepatic IR, due to impaired insulin receptor substrate (IRS) phosphorylation [6], is an increased hepatic glucose production resulting from a failure to suppress gluconeogenesis. Moreover, *de novo* lipid synthesis remains stimulated despite impairment of hepatic insulin signaling [7], leading to fat accumulation within the liver.

In NAFLD patients, some authors found that IR does not influence the progression rate of fibrosis [8], whereas others reported that IR is significantly associated with severe fibrosis [9]. In HCV patients, IR develops early in the course of the disease and precedes steatosis [10]. Moreover, it has been reported that IR is independently associated with histological severity and negatively affects treatment response [11,12]. Supporting the hypothesis that IR could be a pathogenic factor shared by NAFLD and chronic HCV infection, the enhancement of insulin sensitivity improves some clinical and histological features in both liver diseases [13,14].

While there is growing clinical evidence that IR may contribute to disease progression in NAFLD and chronic HCV infection, the extent of impairment of hepatic insulin signaling, the pathways involved, and its impact on liver injury and fibrosis in both conditions remain to be defined. Therefore, the aims of the present study were first to determine the extent of impairment of hepatic insulin signaling and the pathways involved and second, to assess its relationship with liver damage parameters, such as apoptosis and fibrosis in NAFLD and HCV patients. We have also evaluated the effects of lipid accumulation and the HCV *per se* on insulin signaling in cultured human hepatocytes.

Table 1. Demographic, metabolic, biochemical, and histopathological characteristics of patients with normal liver and nonalcoholic fatty liver disease.

Characteristics	NL (n = 29)	NAST (n = 27)	NASH (n = 24)
Age (years)	46.9 ± 10.6	47.1 ± 11.2	47.5 ± 9.7
Women/Men	17(58.6%)/ 12 (41.4%)	16 (59.3%)/ 11 (40.7%)	14 (58.3%)/ 10 (41.7%)
Body mass index (kg/m^2)	25.8 ± 2.7	26.1 ± 2.5	26.4 ± 2.4
Glucose (mg/dl)	89.6 ± 6.5	94.3 ± 9.5	92.1 ± 8.3
Insulin (μU/L)	8.7 ± 4.6	10.9 ± 7.8	11.2 ± 8.1
HOMA-IR	0.96 ± 0.5	1.67 ± 1.1*	1.98 ± 1.6*
Triglycerides (mg/dl)	99.4 ± 26.2	147.3 ± 53.6*	171.5 ± 59.6*
HDL-cholesterol (mg/dl)	49.3 ± 9.7	46.8 ± 12.7	45.3 ± 10.2
Metabolic syndrome (%)	0 (0%)	5 (18.5%)*	7 (29.2%)*
ALT (IU/L)	16.7 ± 5.9	26.3 ± 12.1*	61.8 ± 31.5*#
AST (IU/L)	15.3 ± 6.6	21.3 ± 10.4	37.3 ± 15.6*
γ-GT (IU/L)	27.1 ± 14.6	78.4 ± 53.7*	93.5 ± 62.8*
Steatosis (%)			
Grade 0	29 (100%)		
Grade 1		14 (51.9%)	12 (50.0%)
Grade 2		10 (37.0%)	8 (33.3%)
Grade 3		3 (11.1%)	4 (16.7%)
Fibrosis (%)			
Stage 0	29 (100%)	27 (100%)	6 (25.0%)
Stage 1			9 (37.5%)
Stage 2			6 (25.0%)
Stage 3			3 (12.5%)
Stage 4			
Ballooning and lobular inflammation (%)			
Grade 0	29 (100%)	27 (100%)	
Grade 1			
Grade 2			13 (54.2%)
Grade 3			10 (41.7%)
Grade 4			1 (4.1%)

Data are shown as mean ± standard deviation or as number of cases (%). NL, normal liver; NAST, nonalcoholic steatosis; NASH, nonalcoholic steatohepatitis; HOMA-IR, homeostatic model assessment-insulin resistant; HDL, high-density lipoprotein; ALT, alanine aminotransferase; AST, aspartate aminotransferase; and γ-GT, gamma-glutamyltransferase.*p <0.05 with respect to NL group. #p <0.05 with respect to NAST group.

Patients and methods

Patients

This study comprised 122 nondiabetic patients with a clinical diagnosis of either NAFLD or chronic HCV infection who underwent a liver biopsy with diagnostic purposes. We further studied 29 subjects with histologically normal liver (NL).

Liver tissue studies

Histopathology assessment
Paraffin-embedded liver biopsy sections were evaluated by a single hepatopathologist blinded to the clinical data. Overall, steatosis was assessed as outlined by Brunt *et al.* [15], and the Kleiner's histological scoring [16] was used to evaluate the degree of hepatocellular ballooning and lobular inflammation as well as the stage of fibrosis in NAFLD. Patients with NAFLD were classified into two groups: those with simple steatosis (NAST) and those with definite steatohepatitis (NASH). In the HCV group, the grade of necroinflammation and the stage of fibrosis were scored as proposed by Scheuer [17]. HCV patients were categorized into three groups, depending on whether they were infected with genotype 1(HCV G1) or genotype 3 (HCV G3) and on the presence of steatosis in HCV G1 patients (HCV G1 + NAST).

TUNEL assay
For the detection of apoptosis, the TUNEL commercial kit for cell death detection (Roche Biochemicals, Mannheim, Germany) was used following the instructions of the manufacturer. DAPI was used for DNA staining.

RNA isolation and quantitative real-time PCR analysis
Total RNA of liver biopsy samples from all patients was extracted by using TRIzol reagent (Invitrogen, Carlsbad, CA). Total RNA (1 μg) was reverse transcribed using a SuperScript™ III First-Strand Synthesis System for qPCR following the

Table 2. Demographic, metabolic, biochemical, viral, and histopathological characteristics of patients with chronic hepatitis C virus infection.

Characteristics	HCV G1 (n = 24)	HCV G1+NAST (n = 28)	HCV G3 (n = 19)
Age (years)	47.0 ± 11.1	46.7 ± 10.6	47.2 ± 10.2
Women/Men	14 (58.3%) / 10 (41.7%)	17 (60.7%) / 11 (39.3%)	11 (57.9%) / 8 (42.1%)
Body mass index (kg/m^2)	25.7 ± 2.6	26.3 ± 2.5	25.9 ± 2.7
Glucose (mg/dl)	86.3 ± 10.1	88.1 ± 10.3	87.6 ± 9.7
Insulin (μU/L)	10.5 ± 5.8	10.7 ± 6.6	10.2 ± 5.3
HOMA-IR	1.97 ± 1.2	2.01 ± 1.6	1.64 ± 0.9
Triglycerides (mg/dl)	96.4 ± 41.3	98.1 ± 43.5	95.6 ± 40.2
HDL-cholesterol (mg/dl)	51.1 ± 16.3	50.4 ± 15.2	50.7 ± 13.8
Metabolic syndrome (%)	0 (0%)	0 (0%)	0 (0%)
ALT (IU/L)	105.4 ± 65.1	98.4 ± 57.2	112.7 ± 63.5
AST (IU/L)	59.7 ± 30.5	54.1 ± 34.7	51.9 ± 28.9
γ-GT (IU/L)	39.7 ± 18.4	67.3 ± 38.2*	64.1 ± 33.5*
HCV viral load (%)			
≤ 8.5 x 10^5 IU/ml	7 (29.2%)	9 (32.2%)	6 (31.6%)
> 8.5 x 10^5 IU/ml	17 (70.8%)	19 (67.8%)	13 (68.4%)
Steatosis (%)			
Grade 0	24 (100%)		
Grade 1		19 (67.9%)	12 (63.1%)
Grade 2		6 (21.4%)	4 (21.1%)
Grade 3		3 (10.7%)	3 (15.8%)
Fibrosis (%)			
Stage 0	9 (37.5%)	12 (42.8%)	7 (36.8%)
Stage 1	4 (16.7%)	5 (17.9%)	3 (15.8%)
Stage 2	4 (16.7%)	5 (17.9%)	4 (21.1%)
Stage 3	5 (20.8%)	4 (14.3%)	4 (21.1%)
Stage 4	2 (8.3%)	2 (7.1%)	1 (5.2%)
Necroinflammation (%)			
Grade 0			
Grade 1	7 (29.2%)	8 (28.6%)	4 (21.1%)
Grade 2	11 (45.8%)	12 (42.8%)	10 (52.6%)
Grade 3	6 (25.0%)	8 (28.6%)	5 (26.3%)
Grade 4			

Data are shown as mean ± standard deviation or as number of cases (%). HCV G1, hepatitis C virus genotype 1; HCV G1+NAST, hepatitis C virus genotype 1 with nonalcoholic steatosis; HCV G3, hepatitis C virus genotype 3; HOMA-IR, homeostatic model assessment-insulin resistant; HDL, high-density lipoprotein; ALT, alanine aminotransferase; AST, aspartate aminotransferase; and γ-GT, gamma-glutamyltransferase. *p <0.05 with respect to HCV G1 group.

manufacturer's instructions (Invitrogen). qPCR was performed with an ABI 7900 sequence detector using the SyBr Green method and $d(N)_6$ random hexamer with primers.

Specific primers were purchased from Invitrogen. PCR thermocycling parameters were 95 °C for 10 min, 40 cycles of 95 °C for 15 s, and 60 °C for 1 min. Each sample was run in triplicate and was normalized to 18S RNA. Fold changes were determined using the ΔΔCt method.

Protein extraction and Western blot analysis

Liver biopsy samples from all patients were homogenized in a medium containing: 10 mM Tris–HCl, pH 7.5; 1 mM $MgCl_2$, 1 mM EGTA, 10% glycerol, 0.5% 3-(3-cholamidopropyl) dimethylammonio-1-propanesulfonate (CHAPS), 1 mM-mercaptoethanol, and 0.1 mM PMSF. Extracts were vortexed for 30 min at 4 °C and after centrifuging 20 min at 13,000*g* the supernatants were stored at 80 °C. Protein levels in whole cell lysates were determined with Bradford reagent (BioRadLaboratories, Richmond, CA). Western blot experiments were performed.

Cell culture studies

Plasmid constructs

The expression vector pEF1α has been described previously as pcDEF [18]. The expression vector pEF-core was obtained by subcloning into pEF1α a PCR fragment encoding full-length core protein from HCV genotype 1b.

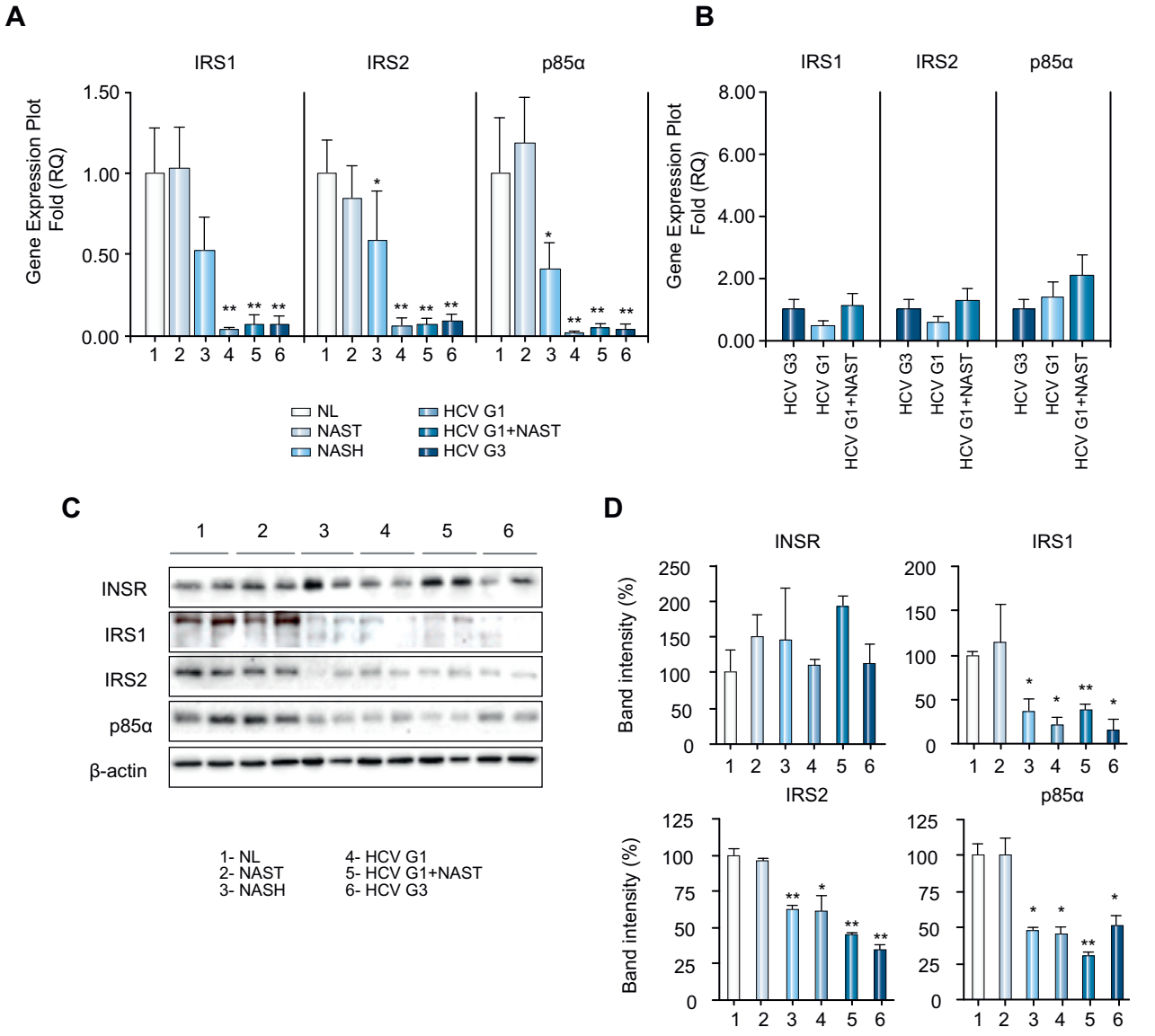

Fig. 1. Hepatic mRNA expression of IRS1, IRS2, and p85α is decreased in NASH and HCV patients. Levels of IRS1, IRS2, and p85α transcripts in liver samples from NL (n = 29), NAST (n = 27), NASH (n = 24), HCV G1 (n = 24), HCV G1 + NAST (n = 28), and HCV G3 (n = 19). (A) Values represent fold relative to NL (1.0). (B) Values represent fold relative to HCV G3 (1.0). (C) Representative Western blotting showing the expression of these proteins. (D) Bar graph shows the mean ± SD of hepatic protein amount in the same study groups. Data are the ratio of a target band density to β-actin band density and are presented as percentage relative to NL (100%). $^{*}p$ <0.05, $^{**}p$ <0.001 *vs.* NL. NL, normal liver; NAST, nonalcoholic steatosis; NASH, nonalcoholic steatohepatitis; HCV G1, hepatitis C virus genotype 1; HCV G1+NAST, hepatitis C virus genotype 1 with nonalcoholic steatosis; HCV G3, hepatitis C virus genotype 3; INSR, insulin receptor.

Stable transfectants

Chang liver (CHL) cells (CCL13; American Type Culture Collection, Manassas, VA) were grown at 37 °C with 5% CO_2 in DMEM supplemented with 10% (v/v) fetal calf serum (BioWhittaker, Walkersville, MD). Polyclonal transfectants CHL-core 1b derived from CHL cells were generated by stably transfecting these cells with the plasmid pEF1α-cDNA EF core 1b as previously described [19]. We also generated transfectants CHL-cat by stable transfection of CHL cells with a vector driving the expression of the bacterial chloramphenicol acetyltransferase (cat) gene, which were used as controls. Where indicated, CHL cells were stimulated with 10 nM insulin (Sigma–Aldrich) for 10 min. Moreover, CHL cells were incubated with culture medium supplemented with 100 μM stearic acid dissolved in isopropanol or with vehicle alone for 24 h either to induce lipid accumulation or to use as controls.

Statistical analysis

Categorical variables are presented as frequency and percentage. Continuous variables are shown as mean ± standard deviation. The baseline characteristics of the patients studied were compared by the Pearson χ^2 test for categorical variables and the unpaired *t* test or Mann–Whitney *U* test for continuous variables. Data from qPCR and Western blotting were compared by using the Kruskal–Wallis ANOVA test. The Spearman's *r*-test was used to evaluate correlations. All statistical analyses were performed using SPSS version 15.0 (SPSS, Cary, NC) software with 2-sided tests, with a p value of <0.05 considered as statistically significant.

Results

Patient characteristics

Characteristics of NAFLD and HCV patients studied are detailed in Tables 1 and 2, respectively. To highlight, all patient groups were well matched in terms of age, sex distribution, and BMI. In the NAFLD cohort, NAST patients had significantly higher mean HOMA-IR score ($p = 0.009$), triglycerides ($p = 0.031$), the rate of metabolic syndrome ($p = 0.017$), ALT ($p = 0.007$), and γ-GT ($p < 0.001$) than subjects with NL. In NASH patients, the mean HOMA-IR score, triglycerides, the frequency of metabolic syndrome; ALT, AST, and γ-GT were significantly higher than in NL individuals ($p = 0.005$, $p = 0.027$, $p < 0.001$, $p < 0.001$, $p = 0.002$ and $p < 0.001$, respectively). Moreover, NASH patients had significantly higher serum ALT levels than NAST patients ($p = 0.013$).

Regarding HCV patients, the lower serum levels of γ-GT in HCV G1 patients than in HCV G1 + NAST and in HCV G3 cohorts ($p = 0.034$ and $p = 0.038$) were the only significant differences among HCV groups.

Hepatic insulin signaling is impaired in NASH and HCV patients

Hepatic mRNA levels of IRS1, IRS2, and p85α were lower in patients with NASH (0.47, 0.41, and 0.59-fold, respectively) than in NL subjects, remaining unchanged in NAST patients (Fig. 1A, left). Furthermore, the expression of these transcripts were significantly decreased in the liver of patients with HCV G1 (0.96, 0.94, and 0.98-fold, respectively), HCV G1 + NAST (0.93, 0.92, and 0.96-fold, respectively), and HCV G3 (0.93, 0.91, and 0.96-fold, respectively) with respect to NL (Fig. 1A, left). When the HCV G3 group was used as control and comparing with HCV G1 and HCV G1 + NAST, no significant differences in the hepatic mRNA levels of IRS1, IRS2, and p85α were found (Fig. 1A, right). Likewise, a decrease in the hepatic protein amount of IRS1, IRS2, and p85α was found in NASH (60%, 38%, and 54%, respectively), HCV G1 (79%, 39%, and 55%, respectively), HCV G1 + NAST (62%, 66%, and 70%, respectively), and HCV G3 (85%, 66%, and 49%, respectively) as compared with NL and NAST patients (Fig. 1B and C). Akt and AMPKα are relevant downstream insulin mediators [20]. As shown in Fig. 2, pAkt/Akt and pAMPKα/AMPKα ratios were decreased in NASH (28% and 56%, respectively), HCV G1 (52% and 62%, respectively), HCV G1 + NAST (59% and 50%, respectively), and HCV G3 (78% and 59%, respectively) but not in NAST patients compared with NL. Next, we analyzed the expression and phosphorylation of the insulin-induced transcription factor FoxO1 [21]. The hepatic content of $pSer^{256}$-FoxO1, when compared with NAST and NL, was significantly lower in NASH, HCV G1, HCV G1 + NAST, and HCV G3.

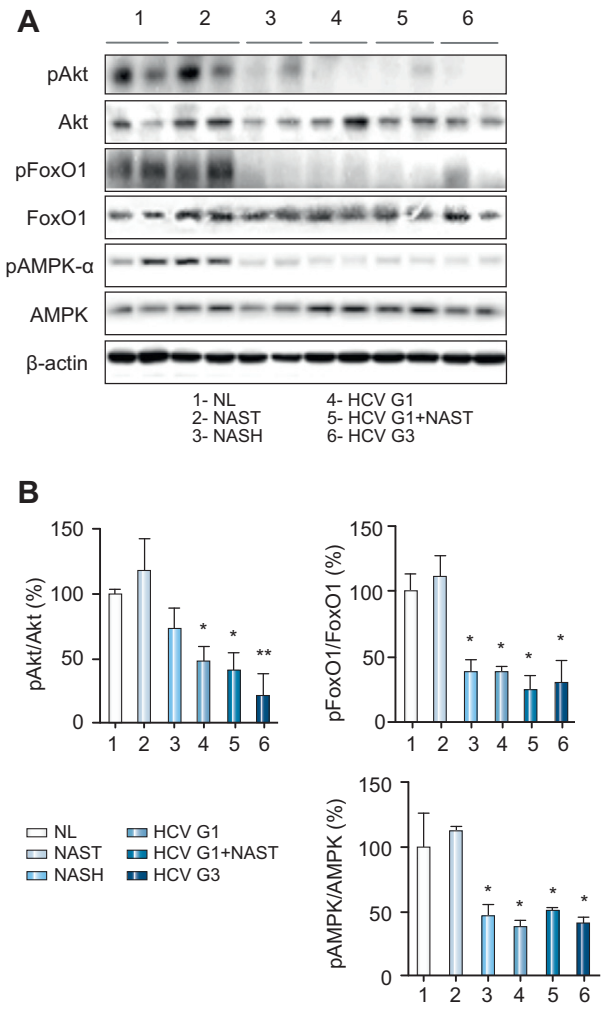

Fig. 2. Hepatic insulin signaling is impaired in NASH and HCV patients. (A) Representative Western blotting showing the level and phosphorylation status of Akt, FoxO1, and AMPK α proteins. (B) Bar graph shows the mean ± SD of hepatic protein amount in the study groups. Data are the ratio of phospho/total band of each protein and are presented as percentage relative to NL (100%). *$p < 0.05$, **$p < 0.001$ *vs.* NL.

Hepatocyte apoptosis and hepatic fibrogenesis are increased in NASH and HCV patients

In NL and NAST patients, no TUNEL-positive cells were identified whereas scattered TUNEL-positive cells were observed in NASH

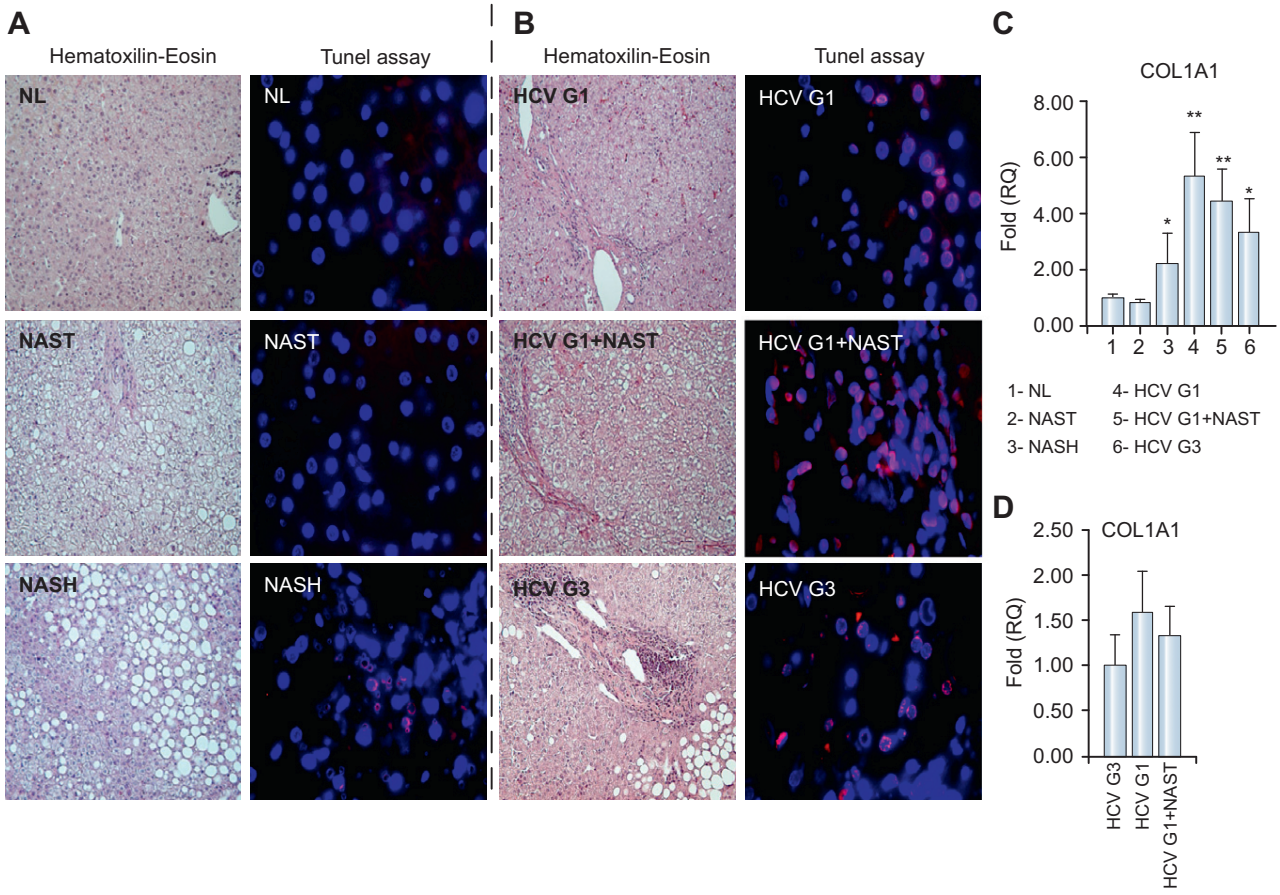

Fig. 3. Increased hepatocyte apoptosis and collagen gene expression in NASH and HCV patients. (A) and (B) Hepatocyte apoptosis (red coloured nuclei) was only observed in NASH and in HCV patient groups. Magnification of hematoxylin–eosin microphotographs: 200×. Magnification of TUNEL microphotographs: 600×. (C) Hepatic mRNA levels of type I collagen (COL1A1) in the study groups. Values represent fold relative to NL (1.0). (D) Values represent fold change relative to HCV G3 (1.0). $^{*}p$ <0.05, $^{**}p$ <0.001 *vs.* NL.

patients (Fig. 3A, left). Of note apoptotic hepatocytes were more frequent in all HCV patient groups (Fig. 3A, right).

Hepatic mRNA levels of collagen α1 (I) (COL1A1) were measured as markers of liver fibrogenesis [22]. When compared with NL, mRNA levels of COL1A1 were similar in NAST but significantly increased in NASH (2.2-fold), HCV G1 (5.3-fold), HCV G1+NAST (4.5-fold), and HCV G3 (3.4-fold) (Fig. 3B, left) but no significant differences were observed among the HCV groups when HCV G3 was used as control (Fig. 3B, right).

On the other hand, compared with NL, hepatic mRNA levels of Mcl-1 and Bcl-2 were significantly diminished in NASH (0.56 and 0.60-fold, respectively), HCV G1 (0.97 and 0.98-fold, respectively), HCV G1+NAST (0.92 and 0.96-fold, respectively), and HCV G3 (0.93 and 0.97-fold, respectively) but not in NAST patients (Fig. 4A, left). When the HCV G3 group was used as control and comparing with HCV G1 and HCV G1+NAST, the expression levels of these transcripts were similar among the distinct HCV groups (Fig. 4A, right). As shown in Fig. 4B and C, the hepatic abundance of Mcl-1 protein was significantly lower in NASH (67%), HCV G1 (56%), HCV G1+NAST (66%), and HCV G3 (67%) than in NL and NAST patients, whereas the amount of Bcl-2 protein was similar among the different patient groups. Moreover, the hepatic content of active caspase 3 was significantly higher in NASH (410%), HCV G1 (330%), HCV G1 + NAST (380%), and HCV G3 (380%) than in NL and NAST patients.

Hepatic expression of insulin signaling genes correlates with antiapoptotic and fibrogenic genes in NASH and HCV patients

A positive correlation was found between hepatic mRNA levels of IRS1 and those of Mcl-1 and Bcl-2 in patients with NASH, whereas a negative correlation was observed with COL1A1 in the same patients (Fig. 5). Regarding HCV patients, a positive correlation was also found between hepatic mRNA levels of IRS1 and those of Mcl-1 and Bcl-2 in patients with HCV G1, HCV G1+NAST, and HCV G3, whereas a negative correlation was observed with COL1A1 in the same patient groups (Fig. 6). Similar correlations have been found with IRS2 and p85α.

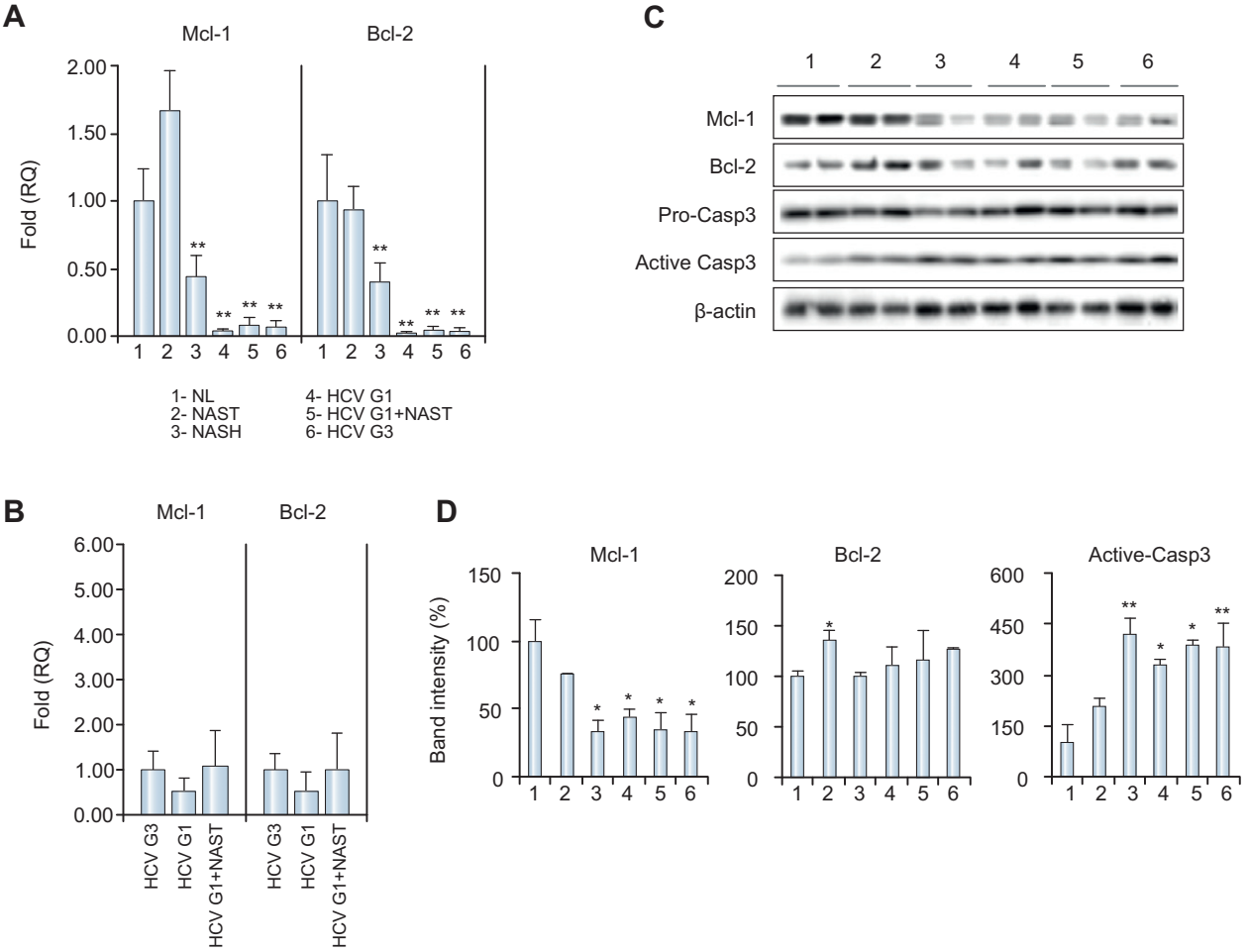

Fig. 4. Intrahepatic expression of antiapoptotic and proapoptotic mediators in NAFLD and HCV patients. Transcript levels of the antiapoptotic genes Mcl-1 and Bcl-2 in liver samples from the different patient groups. (A) Values represent fold change relative to NL (1.0). (B) Values represent fold change relative to HCV G3 (1.0). (C) Representative Western blots showing the hepatic content of Mcl-1, Bcl-2, pro-caspase 3 (Pro-Casp3), and active caspase 3 (Active Casp3). (D) Bar graph shows the mean ± SD of hepatic protein amount in the same study population. Data are the ratio of a target band density to β-actin band density and are presented as a percentage relative to NL (100%). $^{*}p$ <0.05, $^{**}p$ <0.001 *vs.* NL.

HCV core protein induced insulin resistance in cultured human liver cells

After stimulation with 10 nM insulin for 10 min, the phosphorylation of Akt at Ser^{473} was significantly decreased in human hepatocytes transfected with HCV core protein as compared with control cat-transfected cells (Fig. 7). Moreover, incubation of HCV-transfected cells with 100 μM stearic acid for 24 h further reduced insulin-mediated Akt phosphorylation. In addition, we observed that HCV core overexpression increased the phosphorylation of c-Jun N-terminal kinase (JNK) and IRS1 at Ser^{312} (2.5-fold in both cases with respect to control cells). A noteworthy observation was the finding that JNK phosphorylation was significantly enhanced in these cells (6.0-fold higher than controls) when they were incubated for 24 h with stearic acid before insulin stimulation. Finally, using an identical experimental protocol, we obtained similar results regarding the effect of HCV NS5A protein on the phosphorylation levels of Akt and JNK in cultured human hepatocytes (data not shown).

Discussion

The current study demonstrates that hepatic mRNA and protein levels of insulin signaling molecules are significantly decreased in NASH and in HCV patients with or without steatosis and regardless of viral genotype, whereas these parameters are unchanged in NAST with respect to NL individuals. These observations indicate that the hepatic insulin signaling cascade is normal in patients with simple steatosis, favouring the notion that hepatic fat accumulation precedes disruption of hepatic insulin signaling at the molecular level. Furthermore, our results show that the insulin signaling pathway is clearly impaired in patients with steatohepatitis, reinforcing our assumption that downregulation of hepatic insulin mediators is a late event in NAFLD outcome. However, there are contradictory data concerning the relationship between NAFLD and hepatic IR. While clinical studies and animal models indicate that fatty liver may directly induce hepatic IR [23,24], there is increasing evidence against this concept as shown in mice overexpressing the *DGAT*

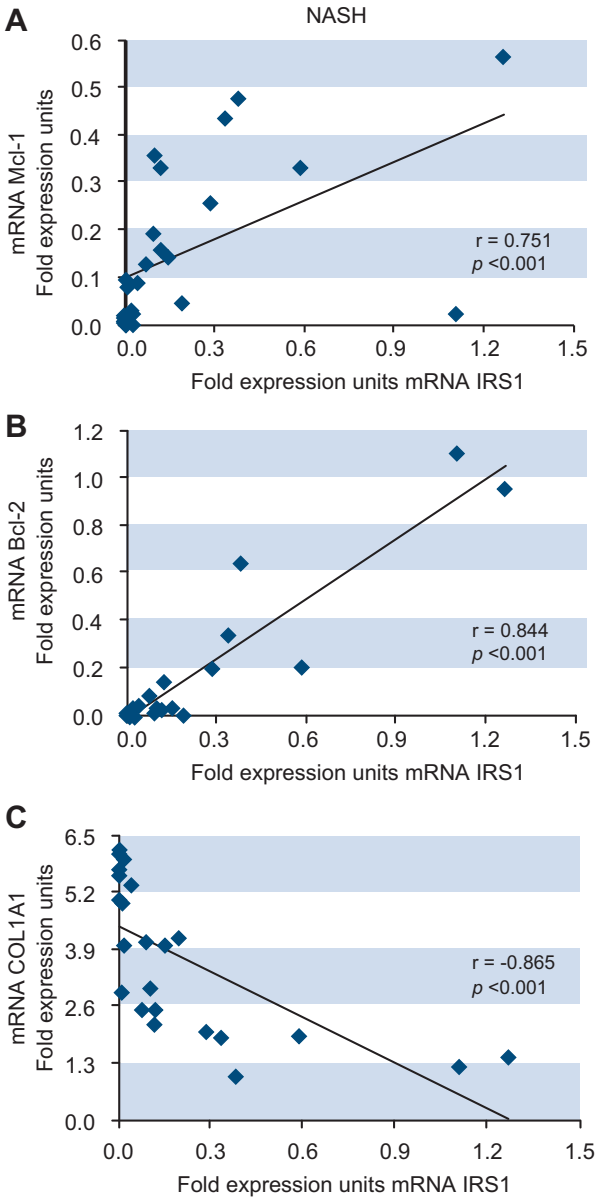

Fig. 5. Hepatic mRNA levels of IRS1 correlate with levels of antiapoptotic and fibrogenic genes in NASH patients. (A–C) Correlations in the cohort of NASH patients ($n = 24$) with matched mRNA values for the genes tested.

gene [25] and in mice with a siRNA-mediated knockdown of the *ECHS1* gene in the liver [26], which develops hepatic steatosis without IR. Subjects with fatty liver and normal insulin sensitivity who bore a single nucleotide polymorphism in the *DGAT2* [27] and *PNPLA3* [28] genes also develop hepatic steatosis without IR. These divergent results are likely related to the variability of animal models and NAFLD patients because of environmental and genetic factors and also can be due to the different methods used for hepatic IR assessment. In this regard, only one study evaluating hepatic IR at the gene expression level in a small cohort of NAFLD patients has been published so far [29]. These authors found that insulin signaling mediators, such as pAkt and pFoxO1, were significantly decreased in NASH patients with respect to NL subjects, remaining unchanged or slightly downregulated in patients with simple steatosis. These findings are in agreement with our present results, supporting the hypothesis that the impairment of insulin signaling in the liver likely occurs via the effects of oxidative stress and cytokine release, both common pathogenic features of NASH [4].

On the other hand, although we have observed a trend to lower HOMA-IR values in HCV G3 patients than in those with HCV G1, hepatic insulin signaling was impaired at a similar extent in both groups of HCV patients regardless of the presence of steatosis, in line with previous reports supporting a direct role of HCV in the development of IR [11,30]. It is well known that tyrosine-phosphorylated IRS1 is an upstream mediator of Akt activation [31] whereas serine phosphorylation negatively modulates IRS1-mediated insulin signaling [32]. Moreover, JNK phosphorylates human IRS1 at the Ser^{312} residue, thereby blocking its tyrosine phosphorylation and, consequently, Akt-mediated insulin signaling [33]. Our *in vitro* data show a significant increase in JNK and IRS1 Ser^{312} phosphorylation by overexpression of the HCV core protein in human hepatocytes accompanied with a significant decrease in Akt phosphorylation. These results and others recently reported [34] suggest that hepatic IR in HCV patients could be due, at least in part, to the increased phosphorylation of JNK in HCV-infected hepatocytes that impair the downstream Akt-signaling pathway, identifying JNK as a potential molecular target of HCV-induced IR.

Although increased hepatocyte apoptosis is now considered as an important factor contributing to liver disease progression in NASH and HCV patients [35,36], the elucidation of the underlying molecular mechanisms is still an active field of research. The present study confirms by TUNEL assay the occurrence of increased hepatocyte apoptosis in NASH and HCV patients, and extends these observations by demonstrating a significant decrease of hepatic mRNA levels of Bcl-2 and Mcl-1, both key antiapoptotic mediators, as well as a significant increase of active caspase 3, the final executor of apoptosis, in NASH and HCV patients with respect to NAST and NL subjects. In addition, we observed a positive correlation between the hepatic mRNA levels of IRS1, IRS2, p85α, and antiapoptotic mediators, indicating that impairment of the hepatic insulin signaling pathway is closely associated with enhanced hepatocyte apoptosis in NASH and HCV patients. This is a novel finding in line with the notion that insulin exerts antiapoptotic functions in many cell types [37]. In particular, we have reported that IRS2 plays an essential role in mediating the antiapoptotic action of insulin in mouse hepatocytes [38]. Thus, it is conceivable that the low hepatic levels of IRS1/2 proteins found in NASH and HCV patients might explain, at least in part, the enhanced hepatocyte apoptosis observed in these patients.

A number of clinical studies suggest that IR is associated with fibrosis progression in NAFLD and HCV patients [9,11]. However, since fibrogenesis is a complex and dynamic process [39], histological analysis of fibrosis stage is unsuitable to evaluate active fibrogenesis. To our knowledge, the current study is the first work measuring insulin signaling targets along with type I collagen gene levels in liver biopsies from NAFLD and HCV patients. Our results show a negative correlation between hepatic mRNA levels

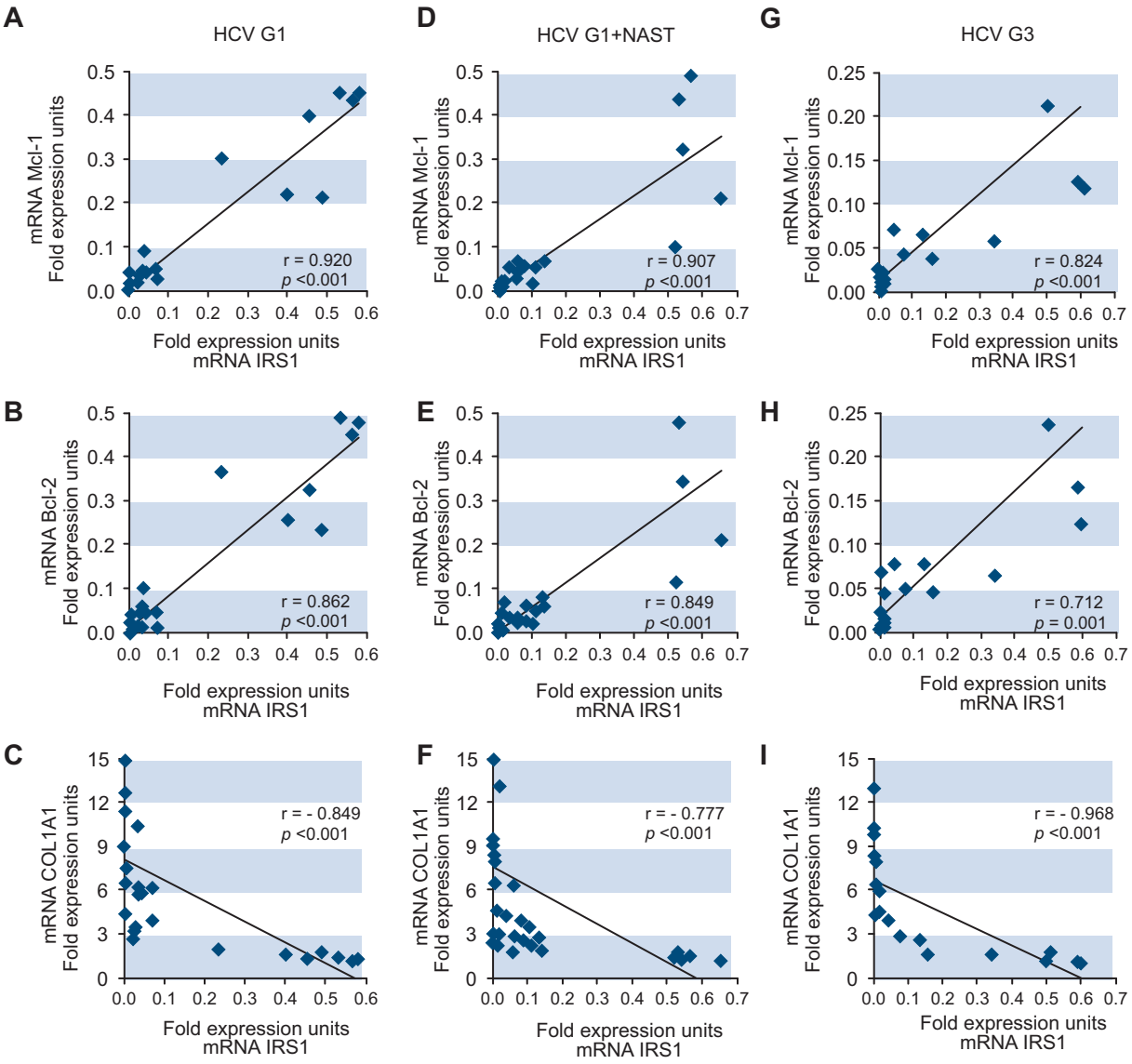

Fig. 6. Hepatic mRNA levels of IRS1 correlate with those of antiapoptotic and fibrogenic genes in HCV patients. (A–C) Correlations in the cohort of HCV G1 patients ($n = 24$) with matched mRNA values for the genes tested. (D) and (F) Correlations in the cohort of HCV G1+NAST patients ($n = 28$) with matched mRNA values for the genes tested. (G)–(I) Correlations in the cohort of HCV G3 patients ($n = 19$) with matched mRNA values for the genes tested.

of IRS1, IRS2, and p85α, and type I collagen showing that disruption of hepatic insulin signaling is associated with increased liver fibrogenesis in both conditions. Plausible mechanisms exist to explain a potential role of hepatic IR in fibrogenesis. Enhanced apoptosis associated with hepatic IR, as we have shown herein, may lead to activation of hepatic stellate cells (HSC) either by the engulfment of apoptotic cells [40] or by a direct effect of Kupffer cells following phagocytosis of apoptotic bodies [41]. In addition, IR-related hyperinsulinemia can stimulate HSC to proliferate and secrete type I collagen [42]. Our present data along with others showing that amelioration of IR improved hepatic fibrosis in NASH and HCV patients suggest that hepatic IR may contribute to fibrogenesis in both entities.

In conclusion, this study demonstrates that hepatic insulin signaling is markedly impaired in NASH and HCV patients, and downregulation of hepatic insulin mediators is associated with enhanced hepatocyte apoptosis and fibrogenesis in both conditions. Moreover, we show that increased phosphorylation of JNK is involved in HCV-induced IR. Our data provide a rationale to address the effect of interventions aimed to improve hepatic insulin sensitivity in attenuating liver injury and fibrosis progression in these chronic liver diseases.

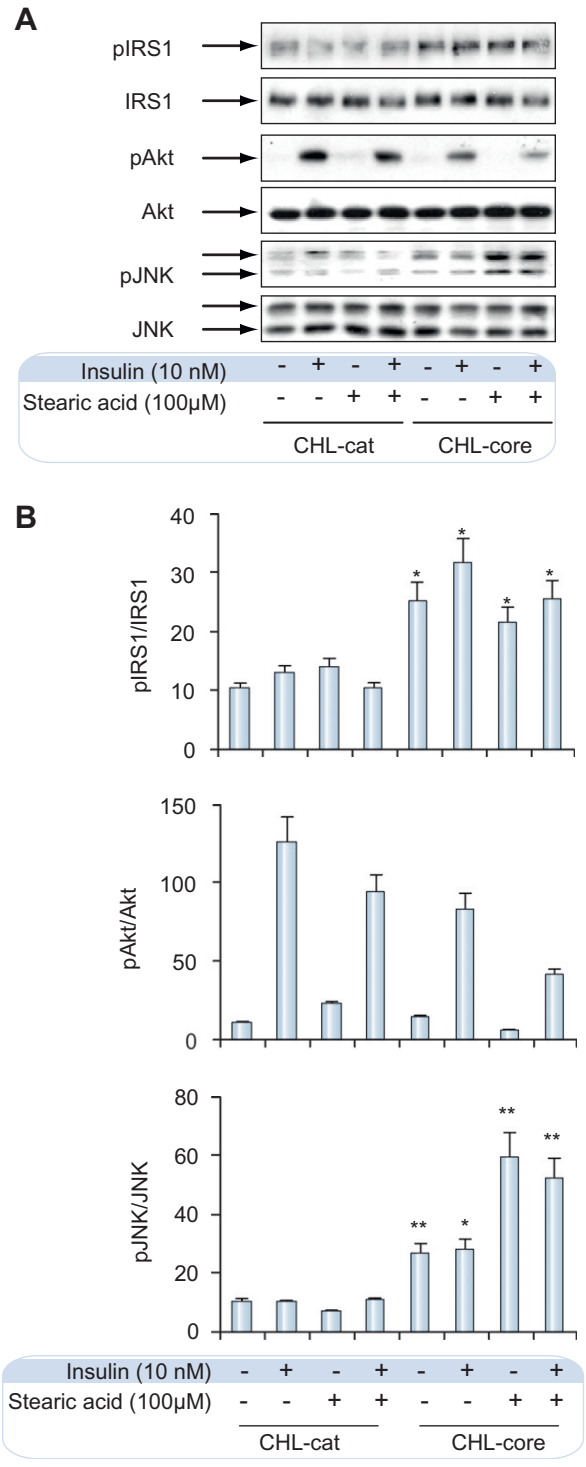

Fig. 7. Insulin signaling is impaired in HCV core-transfected human hepatocytes. (A) Representative Western blots of IRS1 and pIRS1 at Ser^{312}, Akt and pAkt at Ser^{473}, and JNK and pJNK at Thr^{183}/Tyr^{185} (pJNK) in stablytransfected CHL cells under distinct experimental conditions. (B) Values show the mean ± SD of three independent experiments and are expressed as the ratio of phosphorylated/total bands. $^{*}p$ <0.05, $^{**}p$ <0.001 *vs.* corresponding experimental points in CHL-cat cells. HCV, hepatitis C virus; CHL-cat, chloramphenicol acetyltransferase-transfected Chang liver cells; CHL-core, HCV core-transfected Chang liver cells.

Financial disclosure

This work was supported by grants to CG-M from Instituto de Salud Carlos III (PI06/0221 and PI10/0067) and Fundación Eugenio Rodríguez Pascual, Spain; to MCP, AMV and PMS from Ministerio de Ciencia e Innovación (SAF2006-06760), (SAF2009-08114) and (SAF2007-60551), respectively. TL-R and LG-P were supported by CIBERehd contracts. RM-M and AG-R were supported by a CSIC and CIBERdem contract, respectively. CIBERehd and CIBERdem are funded by the Instituto de Salud Carlos III, Spain.

Conflict of interest

The authors who have taken part in this study declared that they do not have anything to disclose regarding funding or conflict of interest with respect to this manuscript.

References

[1] Angulo P. Nonalcoholic fatty liver disease. N Engl J Med 2002;346:1221–1231.
[2] Lauer GM, Walker BD. Hepatitis C virus infection. N Engl J Med 2001;345:41–52.
[3] Bugianesi E, McCullough AJ, Marchesini G. Insulin resistance: a metabolic pathway to chronic liver disease. Hepatology 2005;42:987–1000.
[4] Larter CZ, Farrell GC. Insulin resistance, adiponectin, cytokines in NASH: which is the best target to treat? J Hepatol 2006;44:253–261.
[5] Previs SF, Withers DJ, Ren JM, White MF, Shulman GI. Contrasting effects of IRS-1 versus IRS-2 gene disruption on carbohydrate and lipid metabolism in vivo. J Biol Chem 2000;275:38990–38994.
[6] Valverde AM, Burks DJ, Fabregat I, Fisher TL, Carretero J, White MF, et al. Molecular mechanisms of insulin resistance in IRS-2-deficient hepatocytes. Diabetes 2003;52:2239–2248.
[7] Browning JD, Horton JD. Molecular mediators of hepatic steatosis and liver injury. J Clin Invest 2004;114:147–152.
[8] Adams LA, Sanderson S, Lindor KD, Angulo P. The histological course of nonalcoholic fatty liver disease: a longitudinal study of 103 patients with sequential liver biopsies. J Hepatol 2005;42:132–138.
[9] Marchesini G, Bugianesi E, Forlani G, Cerrelli F, Lenzi M, Manini R, et al. Nonalcoholic fatty liver, steatohepatitis, and the metabolic syndrome. Hepatology 2003;37:917–923.
[10] Romero-Gomez M. Insulin resistance and hepatitis C. World J Gastroenterol 2006;12:7075–7080.
[11] Moucari R, Asselah T, Cazals-Hatem D, Voitot H, Boyer N, Ripault MP, et al. Insulin resistance in chronic hepatitis C: association with genotypes 1 and 4, serum HCV RNA level, and liver fibrosis. Gastroenterology 2008;134:416–423.
[12] Romero-Gomez M, Del Mar Viloria M, Andrade RJ, Salmerón J, Diago M, Fernández-Rodríguez CM, et al. Insulin resistance impairs sustained response rate to peginterferon plus ribavirin in chronic hepatitis C patients. Gastroenterology 2005;128:636–641.
[13] Mathurin P, Hollebecque A, Arnalsteen L, Buob D, Leteurtre E, Caiazzo R, et al. Prospective study of the long-term effects of bariatric surgery on liver injury in patients without advanced disease. Gastroenterology 2009;137:532–540.
[14] Everhart JE, Lok AS, Kim HY, Morgan TR, Lindsay KL, Chung RT, et al. Weight related effects on disease progression in the hepatitis c antiviral long-term treatment against cirrhosis trial. Gastroenterology 2009;137:549–557.
[15] Brunt EM, Janney CG, Di Bisceglie AM, Neuschwander-Tetri BA, Bacon BR. Nonalcoholic steatohepatitis: a proposal for grading and staging the histological lesions. Am J Gastroenterol 1999;94:2467–2474.
[16] Kleiner DE, Brunt EM, Van Natta M, Behling C, Contos MJ, Cummings OW, et al. Design and validation of a histological scoring system for nonalcoholic fatty liver disease. Hepatology 2005;41:1313–1321.
[17] Scheuer PJ. Classification of chronic viral hepatitis: a need for reassessment. J Hepatol 1991;13:372–374.
[18] Zhu N, Khoshnan A, Schneider R, Matsumoto M, Dennert G, Ware C, et al. Hepatitis C virus core protein binds to the cytoplasmic domain of tumor

necrosis factor (TNF) receptor 1 and enhances TNF-induced apoptosis. J Virol 1998;72:3691–3697.
[19] Núñez O, Fernández-Martínez A, Majano PL, Apolinario A, Gómez-Gonzalo M, Benedicto I, et al. Increased intrahepatic cyclooxygenase 2, matrix metalloproteinase 2, and matrix metalloproteinase 9 expression is associated with progressive liver disease in chronic hepatitis C virus infection: role of viral core and NS5A proteins. Gut 2004;53:1665–1672.
[20] Long YC, Zierath JR. AMP-activated protein kinase signalling in metabolic regulation. J Clin Invest 2006;116:1776–1783.
[21] Frescas D, Valenti L, Accili D. Nuclear trapping of the forkhead transcription factor FoxO1 via Sirt-dependent deacetylation promotes expression of glucogenetic genes. J Biol Chem 2005;280:20589–20595.
[22] Bataller R, Brenner DA. Liver fibrosis. J Clin Invest 2005;115:209–218.
[23] Marchesini G, Brizi M, Bianchi G, Tomassetti S, Bugianesi E, Lenzi M, et al. Nonalcoholic fatty liver disease: a feature of the metabolic syndrome. Diabetes 2001;50:1844–1850.
[24] Samuel VT, Liu ZX, Qu X, Elder BD, Bilz S, Befroy D, et al. Mechanism of hepatic insulin resistance in non-alcoholic fatty liver disease. J Biol Chem 2004;279:32345–32353.
[25] Monetti M, Levin MC, Watt MJ, Sajan MP, Marmor S, Hubbard BK, et al. Dissociation of hepatic steatosis and insulin resistance in mice overexpressing DGAT in the liver. Cell Metab 2007;6:69–78.
[26] Zhang X, Yang J, Guo Y, Ye H, Yu C, Xu C, et al. Functional proteomic analysis of nonalcoholic fatty liver disease in rat models: Enoyl–Coenzyme A hydratase down-regulation exacerbates hepatic steatosis. Hepatology 2010;51:1190–1199.
[27] Kantartzis K, Machicao F, Machann J, Schick F, Fritsche A, Häring HU, et al. The DGAT2 gene is a candidate for the dissociation between fatty liver and insulin resistance in humans. Clin Sci (Lond.) 2009;116:531–537.
[28] Kantartzis K, Peter A, Machicao F, Machann J, Wagner S, Königsrainer I, et al. Dissociation between fatty liver and insulin resistance in humans carrying a variant of the patatin-like phospholipase 3 gene. Diabetes 2009;58:2616–2623.
[29] Valenti L, Rametta R, Dongiovanni P, Maggioni M, Francanzani AL, Zappa M, et al. Increased expression and activity of the transcription factor FOXO1 in nonalcoholic steatohepatitis. Diabetes 2008;57:1355–1362.
[30] Shintani Y, Fujie H, Miyoshi H, Tsutsumi T, Tsukamoto K, Kimura S, et al. Hepatitis C virus infection and diabetes: direct involvement of the virus in the development of insulin resistance. Gastroenterology 2004;126:840–848.
[31] Fisher TL, White MF. Signalling pathways: the benefits of good communication. Curr Biol 2004;14:R1005–R1007.
[32] Morino K, Petersen KF, Shulman GI. Molecular mechanisms of insulin resistance in humans and their potential links with mitochondrial dysfunction. Diabetes 2006;55:S9–S15.
[33] Solinas G, Naugler W, Galimi F, Lee MS, Karin M. Saturated fatty acids inhibit induction of insulin gene transcription by JNK-mediated phosphorylation of insulin-receptor substrates. Proc Natl Acad Sci USA 2006;103:16454–16459.
[34] Banerjee S, Saito K, Ait-Goughoulte M, Meyer K, Ray RB, Ray R. Hepatitis C virus core protein upregulates serine phosphorylation of insulin receptor substrate-1 and impairs the downstream akt/protein kinase B signalling pathway for insulin resistance. J Virol 2008;82:2606–2612.
[35] Feldstein AE, Canbay A, Angulo P, Taniai M, Burgart LJ, Lindor KD, et al. Hepatocyte apoptosis and fas expression are prominent features of human nonalcoholic steatohepatitis. Gastroenterology 2003;125:437–443.
[36] Walsh MJ, Vanags DM, Clouston AD, Richardson MM, Purdie DM, Jonsson JR, et al. Steatosis and liver cell apoptosis in chronic hepatitis C: a mechanism for increased liver injury. Hepatology 2004;39:1230–1238.
[37] Navarro P, Valverde AM, Benito M, Lorenzo M. Insulin/IGF-I rescues immortalized brown adipocytes from apoptosis down-regulating Bcl-xS expression, in a PI 3-kinase and MAP kinase-dependent manner. Exp Cell Res 1998;243:213–221.
[38] Valverde AM, Fabregat I, Burks DJ, White MF, Benito M. IRS-2 mediates the antiapoptotic effect of insulin in neonatal hepatocytes. Hepatology 2004;40:1285–1294.
[39] Friedman SL. Mechanisms of hepatic fibrogenesis. Gastroenterology 2008;134:1655–1669.
[40] Canbay A, Taimr P, Torok N, Higuchi H, Friedman S, Gores GJ. Apoptotic body engulfment by a human stellate cell line is profibrogenic. Lab Invest 2003;83:655–663.
[41] Canbay A, Feldstein AE, Higuchi H, Werneburg N, Grambihler A, Bronk SF, et al. Kupffer cell engulfment of apoptotic bodies stimulates death ligand and cytokine expression. Hepatology 2003;38:1188–1198.
[42] Svegliati-Baroni G, Ridolfi F, Di Sario A, Casini A, Marucci L, Gaggiotti G, et al. Insulin and insulin-like growth factor-1 stimulate proliferation and type I collagen accumulation by human hepatic stellate cells: differential effects on signal transduction pathways. Hepatology 1999;29:1743–1751.